



# Comparison of Fe/Al<sub>2</sub>O<sub>3</sub> and Fe, Co/Al<sub>2</sub>O<sub>3</sub> Catalysts Used for Production of Carbon Nanotubes From Acetylene by CCVD

Zoltán Kónya, István Vesselényi, Károly Lázár, János Kiss, and Imre Kiricsi

**Abstract**—Characterization of iron containing alumina supported catalysts was performed by transmission electron microscopy (TEM), Mössbauer, and XPS spectroscopy during formation of multiwall carbon nanotubes from acetylene at 1000 K. TEM images showed that carbon fibers (outer diameter is around 20–40 nm) were generated on Fe/Al<sub>2</sub>O<sub>3</sub> samples while on the bimetallic Fe,Co/Al<sub>2</sub>O<sub>3</sub> carbon nanotubes with an average diameter of 8–12 nm were formed. XPS spectra revealed that Fe–Co alloy formed during the interaction of Fe,Co/Al<sub>2</sub>O<sub>3</sub> and acetylene at 1000 K. The formation of the bimetallic alloy was proven by Mössbauer spectroscopy as well.

**Index Terms**—Iron containing alumina supported catalyst, nanotubes, Mössbauer spectroscopy, XPS spectroscopy.

## I. INTRODUCTION

SINCE their discovery in 1991 [1], carbon nanotubes have been generating a continuously growing interest since these hollow nanostructures have exceptional electrical [2] and mechanical [3] properties, making them usable in many fields. Various production methods have been developed aiming at the production of carbon nanotubes in large scale. Of the main synthetic processes, laser vaporization [4], electric arc discharge [5], and catalytic chemical deposition of hydrocarbons over metal catalysts (CCVD technique) [6], only the latter method supplies carbon nanotubes in high yield at a low cost of production. Being a catalytic process, the combinations of transition metals and supports can be changed depending on the characteristics required, for example, the alignment [7] or the size of the tubes [8], [9]. On the other hand, it has been demonstrated that supported transition metals (in particular iron, cobalt, and nickel) on silica [10], alumina [11], zeolite- and clay-derived [%BIBREFGournis:2002%] supports are used frequently in this process [12]. For characterizing and comparing the productivity of the catalysts the amount of

produced carbon can be related to the amount of pristine catalyst [13]. Beside the amount of the product, the quality of carbon tubes should also be evaluated, mostly transmission electron microscopy (TEM) is used for this. In addition, as an indirect method, thermogravimetry (TG) can also be used; since the ignition temperature of amorphous carbon (the primary by-product) is smaller than that of the graphitic carbon [from which the walls of multiwall nanotubes (MWNTs) are formed] [14].

Iron-base catalysts usually produce carbonaceous tubes with high efficiency. However, as high-resolution electron microscopy studies reveal, the MWNTs may be covered with amorphous carbon in significant extents, i.e., the product is not always pure MWNT. To improve the catalyst performances, supported bimetallic systems composed from Fe, Co, and Ni (2.5 wt% each) were also prepared and evaluated. Fe–Co systems were found to produce MWNTs with superior quality and yields on various supports (alumina, 13X, and ZSM-5 zeolites) [15], or on mixtures of them (silica-aluminas) [16].

In the present paper, for interpreting the advantageous effect of alloying Fe with Co, a report is given on the characterization of the alumina supported fresh and spent Fe-, and Fe co-catalysts. Samples were analyzed by Mössbauer and infrared (IR) spectroscopies, XPS and X-ray diffraction (XRD). The formed carbonaceous products were characterized by TEM and TG techniques, as well.

## II. EXPERIMENTAL

Preparation of the catalysts is described in detail in a previous paper [16]. Briefly, the alumina prepared from aluminum isopropoxide, was impregnated with iron(II)-acetate solution containing iron in an appropriate concentration to obtain catalyst with 2.5% iron content. The bimetallic sample was prepared similarly using cobalt(II)-acetate and iron(II)-acetate solutions. The sum of metal content was 5 w%.

Catalysts were layered on a quartz boat and placed into a horizontal tubular reactor. Preceding the reaction of acetylene, catalysts were treated in nitrogen flow at 473 K, for 1 h, followed by heating to the reaction temperature. At 1000 K, the nitrogen flow was switched for nitrogen–acetylene gas mixture to start the CCVD reaction. After 30 min, the acetylene was stopped and the catalyst was cooled to ambient temperature while nitrogen was flushing the reactor. Then, the mixture of the catalyst and the product was transferred to a dry box with exclusion of air. In the dry box, the mixture was impregnated with molten wax.

Manuscript received June 12, 2003; revised November 3, 2003. This work was supported in part by the National Science Foundation of Hungary under Contracts OTKA T037952 and F038249. The work of Z. Kónya was supported in part by the Magyary Zoltan Research Fellowship. This paper was presented in part at the Symposium of Microtechnologies for the New Millennium, Nanotechnology Conference, Gran-Canaria, Spain, May 2003.

Z. Kónya, I. Vesselényi, and I. Kiricsi are with the Department of Applied and Environmental Chemistry, University of Szeged, H-6720 Szeged, Hungary.

K. Lázár is with the Chemical Research Center of the Hungarian Academy of Sciences, Institute of Isotope and Surface Chemistry, H-1525 Budapest, Hungary.

J. Kiss is with the Reaction Kinetics Research Group of the Hungarian Academy of Sciences, University of Szeged, H-6701 Szeged, Hungary.

Digital Object Identifier 10.1109/TNANO.2004.824033

After solidifying the sample, a wafer was obtained in which the metal particles were isolated from air, providing thereby semi *in situ* conditions for the further characterization.

XRD patterns were obtained on a DRON 3 diffractometer operated under computer control. XRD profiles were registered in the 3–60  $2\theta$  range using Cu  $K_{\alpha}$  radiation.

For IR spectroscopic study the KBr matrix wafer technique was applied. 1 mg of sample from the different stages of treatments was mixed with 100 mg KBr of spectroscopic purity. Pellets were pressed from the mixtures and their spectra were recorded with the Mattson Genesis 1 FTIR spectrometer.

Thermal behavior of the catalyst samples used for production of carbon nanotubes were tested using a method-of-moments (MOM) Derivatograph Q instrument. Thermal analytical features were recorded in the 300–1300 K temperature range. A 100 mg of sample was placed into a ceramic sample holder and tested while the temperature was increased from 300 to 1300 K with a ramp of 10 K/min.

Mössbauer spectra were recorded on a KFKI spectrometer in constant acceleration mode at ambient and 77 K (liquid nitrogen) temperatures. Positional parameters are related to metallic  $\alpha$ -iron, their estimated accuracy is  $\pm 0.03$  mm/s. The characteristic Mössbauer parameters were determined by decomposing the spectra to Lorentzian lines.

The XPS experiments were performed in an ultrahigh vacuum system with a background pressure of  $10^{-9}$  mbar, produced by an iongetter pump. The photoelectrons generated by Al  $K_{\alpha}$  primary radiation (15 kV, 15 mA) were analyzed with a hemispherical electron energy analyzer (Kratos XSAM 800). The pass energy was set to 40 eV. An energy step width of 50 meV and a dwell time of 300 ms were used. Typically, 10 scans were accumulated for each spectrum. Fitting and deconvolution of the spectra were performed with the help of VISION software. All binding energies were referenced to Al(2p) at 74.7 eV.

Before measurements, the sample was evacuated at 300 K and calcined at 1000 K for 20 min in the sample preparation chamber, which was connected directly to the analyzing chamber by a sample transfer system. In the sample preparation chamber, the catalyst can be heated up to 1100 K in various gas atmospheres (in the present case in acetylene–nitrogen mixture).

Approximately 1 mg of product was homogenized in 10 ml ethanol for 30 min, using ultrasonic treatment. A few drops of the resulting suspension were put on a carbon film coated TEM grid. TEM images were taken by a Philips CM 20 electron microscope.

### III. RESULTS AND DISCUSSION

#### A. Infrared Spectroscopy

The IR spectra of catalysts treated in nitrogen at 1000 K show no band due to decomposition residues of acetate salts. The reaction of catalyst in acetylene stream gives rise bands neither due to surface OH groups nor to CH residues. This reveals that product contains exclusively high purity carbon and not carbonaceous compounds having hydrogen. (More precisely, the

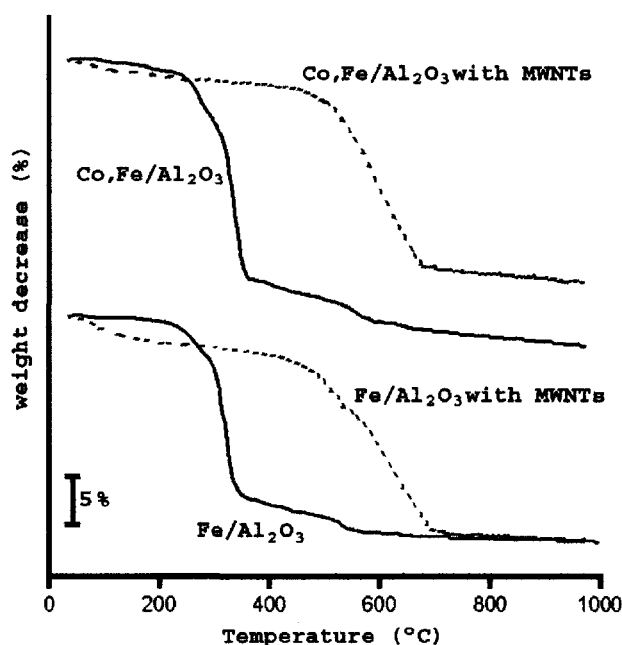


Fig. 1. Derivatographic patterns of the catalysts before and after reaction.

concentration of CH groups falls below the detection limit of IR spectroscopy).

#### B. Thermogravimetry

Derivatographic patterns for the fresh and the spent catalyst samples are seen in Fig. 1. The TG and DTG curves of starting specimens show three weight loss steps both for the iron and for the cobalt-iron materials. Both the temperatures and the weight losses due to the respective steps are very similar. The values are listed in Table I.

#### C. XRD

Fig. 2 shows the XRD patterns of samples after different treatments. After impregnating the alumina support with the metal salts several peaks can be found on the XRD spectra for both the mono- and the bimetallic catalysts [Fig. 2 (a)]. These peaks can be assigned as iron(II)-acetate and cobalt(II)-acetate.

No peaks are shown in the XRD pattern in the 3–50°  $2\theta$  range of the Fe-AlOH sample treated at 1000 K in pure nitrogen atmosphere [Fig. 2(b)–Fe]. In contrast, the bimetallic sample treated identically exhibits a rather sharp peak at 42°  $2\theta$  in the diffractogram [Fig. 2(b)–CoFe].

XRD profiles registered on the acetylene treated samples show several changes compared to the simple heat treated reference samples [Fig. 2(c) spectra]. First, broad signals due to the graphitic carbon nanotubes are seen at 23–25°  $2\theta$ . For Fe-AlOH sample a second broad reflection appears at 45.2°  $2\theta$ . On the feature of bimetallic specimen no signal is seen in this region [Fig. 2(c)–CoFe]. The reflection additional to the signal of nanotubes is situating at the same place as for the heat treated sample, however, its intensity is much smaller.

TABLE I  
SUMMARY OF THE RESULTS OBTAINED BY DERIVATOGRAPHY

Fe-AlOH (fresh)		Fe-AlOH (spent)	
Temperature (°C)	Weight loss (w%)	Temperature (°C)	Weight loss (w%)
248	4.3	164	4.6
327	22.5	443	
515	4.6	591	28

Co,Fe-AlOH (fresh)		Co,Fe-AlOH (spent)	
Temperature (°C)	Weight loss (w%)	Temperature (°C)	Weight loss (w%)
248	7.5	145	3
324	27.5	606	25
520	6	700	1.5

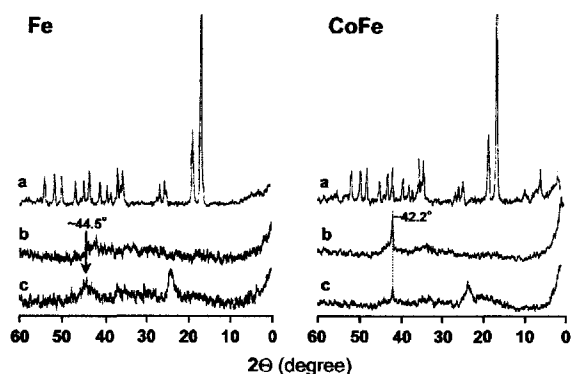


Fig. 2. XRD spectra of the monometallic and the bimetallic catalysts. (a) After impregnation. (b) After calcinations in air. (c) After reaction with acetylene.

#### D. CCVD Reaction

Comparison of the productivity of the two catalyst showed that acetylene decomposed on both samples. However, the quality of carbon formed on the catalyst specimens was different. Carbon formed on the Fe/Al<sub>2</sub>O<sub>3</sub> sample was mostly amorphous. In contrast, carbon produced on the bimetallic sample contained carbon nanotubes in rather high concentration. This present observation is in complete accordance with the literature data [17].

#### E. Characterization by TEM

The product of acetylene decomposition on Fe/Al<sub>2</sub>O<sub>3</sub> showed pure carbon deposit and the carbon nanotube content was rather low, i.e., only few carbon nanotubes were found. Contrary to this, MWNTs were dominated in the deposit formed on Co,Fe/Al<sub>2</sub>O<sub>3</sub> catalyst. Here much less amorphous carbon was detected. Two characteristic TEM images are seen in Fig. 3.

#### F. Mössbauer Spectroscopy

Mössbauer spectra were recorded in two velocity ranges:  $\pm 12$  and  $\pm 8$  mm/s. The spectra of the wider velocity scale clearly demonstrate the transformation of the starting oxide to zerovalent metallic/carbide components as a result of exposure to acetylene during CCVD (Fig. 4). Spectra of converted catalysts were obtained both at ambient and 77 K temperatures (Fig. 5). Data extracted from the spectra are compiled in Table II.

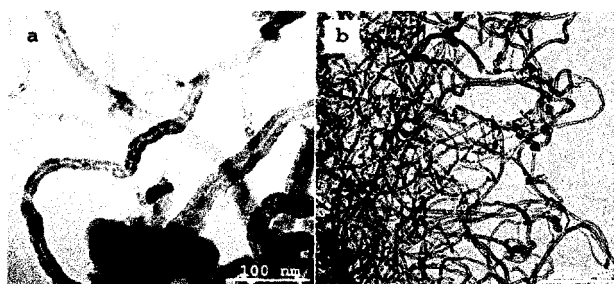


Fig. 3. TEM images of fibers/nanotubes produced on (a) Fe/Al<sub>2</sub>O<sub>3</sub> or (b) Fe,Co/Al<sub>2</sub>O<sub>3</sub>.

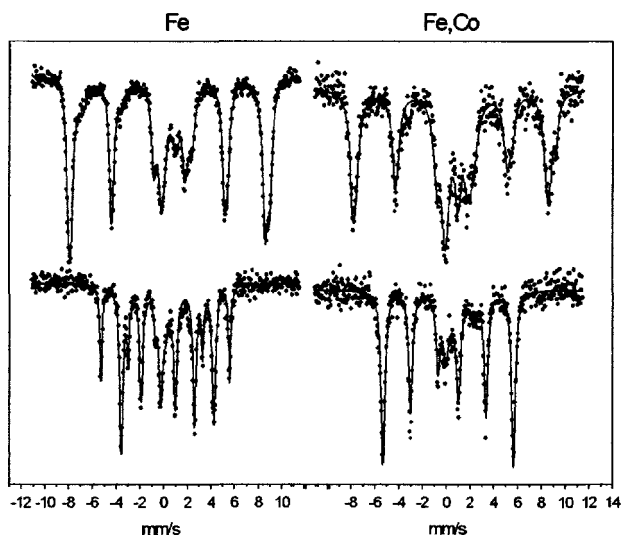


Fig. 4. Mössbauer spectra of fresh (top) and spent (bottom) catalysts recorded at 77 K temperature.

Dominant portions of spectra of fresh catalysts are characteristic for spinel oxides. They exhibit the magnetic sextets of anti-ferromagnetic coupling, and the tetrahedral (A) and octahedral [B] sites can be distinguished. Iron in [B] sites exhibits larger IS and MHF values in comparison to (A) positions [18].

Most of iron in the Fe/Al<sub>2</sub>O<sub>3</sub> sample is located in maghemite ( $\gamma$ -Fe<sub>2</sub>O<sub>3</sub>) structure. In correspondence, (A) and [B] sites display different IS and MHF values (Table II). From the spectrum of the binary Fe,Co/Al<sub>2</sub>O<sub>3</sub> catalyst incorporation of Co into the structure can be revealed: IS increases in [B] sites, the  $\sim 1:1$  ratio in occupation of sites, (A)/[B], is changed to  $\sim 5:2$ , Co ions prefer to occupy [B] positions.

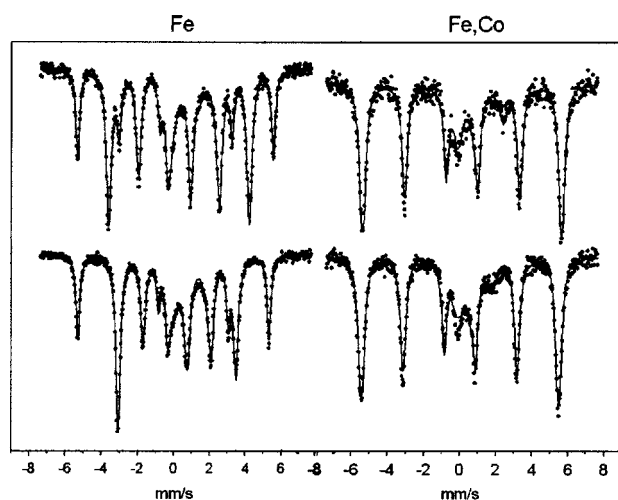


Fig. 5. Mössbauer spectra of spent catalysts recorded at 77 K (top) and at ambient temperature (bottom).

Exposure of the fresh catalysts to the reaction mixture converts the oxides to a zerovalent state: the MHF values drop significantly, i.e., the antiferromagnetic oxides are converted to ferromagnetic particles.

An apparent difference between the  $\text{Fe}/\text{Al}_2\text{O}_3$  and the  $\text{Fe,Co}/\text{Al}_2\text{O}_3$  sample is clearly visible: a sextet indicating a component of a low-magnetic field is present in the spectra of the single-metal  $\text{Fe}/\text{Al}_2\text{O}_3$  catalyst in high proportion (with c.a. half of the spectral area). This low-internal field (24.3 and 20.4 Tesla at 77 and 300 K, respectively) is characteristic for  $\Theta\text{-Fe}_3\text{C}$  [19]. In contrast, no iron carbide is detected in the spectra of bimetallic  $\text{Fe,Co}/\text{Al}_2\text{O}_3$  sample.

Inspection of the spectra of the spent  $\text{Fe,Co}/\text{Al}_2\text{O}_3$  catalyst, reveals a further characteristic difference. The displayed metallic sextets are asymmetric (Fig. 5) and they can be decomposed to two components. The magnetic field shown by the dominant component (in which about half of the iron is involved) is  $\sim 34.4$  Tesla. This value exceeds significantly the value characteristic for pure iron. It can only be attributed to bimetallic alloyed  $\text{Fe,Co}$  particles (since alloying with Co results in the increase of the internal magnetic field [18]). The component present in minor amount exhibits  $\sim 33.5$  Tesla field, it can be attributed to metallic iron. Thus, in short, in the spectra of the spent  $\text{Fe}/\text{Al}_2\text{O}_3$  catalyst the  $\Theta\text{-Fe}_3\text{C}$  component dominates, whereas in the spectra of the  $\text{Fe,Co}/\text{Al}_2\text{O}_3$  catalyst the  $\text{Fe,Co}$  bimetallic alloy is the main constituent.

A further aspect is also worth mentioning: the overwhelming portion ( $\geq 80\%$ ) of the spectra of the spent catalysts is attributed to magnetically ordered components. Considering the fact that a condition for the appearance of magnetic ordering (sextet in a Mössbauer spectrum) is a minimal particle size (6–8 nm [20]), it can also be noted that the size of the particles certainly exceeds the mentioned threshold value.

### G. XPS Spectroscopy Results

After evacuation of a received  $\text{Fe}/\text{Al}_2\text{O}_3$ , the emission of  $2p_{3/2}$  appeared at 711.6 eV, while the  $2p_{1/2}$  was measured at

725.1 eV. The position and energy separation are very close to that observed for the  $\text{FeO}(\text{OH})$  structure [21] and the observed broad shakeup satellite at 719.8 eV is also characteristic of  $\text{Fe}^{3+}$ . Significant changes were observed when the sample was kept at 1000 K in acetylene atmosphere for 60 min. The  $\text{Fe}(2p_{3/2})$  signal shifted to lower binding energy by 1.6 eV, and two satellite appeared at around 713.5 and 718.0 eV [Fig. 6(A)]. The most important observation is that in such a strong reducing atmosphere we could not detect photoemission at 707.0 eV, which is characteristic of bulk metal iron. Under this experimental condition, partially oxidised iron (such as  $\text{Fe}_x\text{O}$ ) should not exist on the catalyst surface. We assume that the higher binding energy indicates that the particle size is small. In the dispersed system, neighboring atoms are fewer than in bulk, therefore, screening electrons are fewer as well. As a consequence, the core-hole screening is less effective and the binding energy of the orbital shifts to higher energy. This effect could operate in the present case, too. However, the large binding energy difference could not be explained only this way, because 1000 K is a high enough temperature for the agglomeration of iron particles to occur. The formation of iron-carbide ( $\text{Fe}_2\text{C}$  or  $\text{Fe}_3\text{C}$ ) plays an important role in the position of the observed binding energy, which was shown in the Mössbauer spectra as well.

Fig. 6(B), shows the main photoemission signals of iron in  $\text{Fe,Co}$  bimetallic catalyst before photo reduction and after acetylene treatment at 300 and 1000 K. In the unreduced samples (evacuated at 300 K and sintered at 1000 K), the peak positions were almost the same as for  $\text{Fe}/\text{Al}_2\text{O}_3$ . Acetylene adsorption at 300 K did not cause significant change. When the bimetallic catalyst was exposed to acetylene at 1000 K, the  $\text{Fe}(2p_{3/2})$  signal moved to higher binding energy by 0.4 eV. The same shift was observed for ( $2p_{1/2}$ ), too. When the Fe was alone in the supported catalyst the direction of the shift was the opposite. The formation of the small metallic cluster and mainly the formation of  $\text{Fe}_x\text{C}$  may explain the phenomenon. However, in this case we cannot operate with these assumptions. We attribute these changes to the formation of  $\text{Fe-Co}$  alloy. It is important to mention that similar shift was observed for  $\text{Fe,Co}/\text{TiO}_2$  bimetallic catalyst after reduction [22].

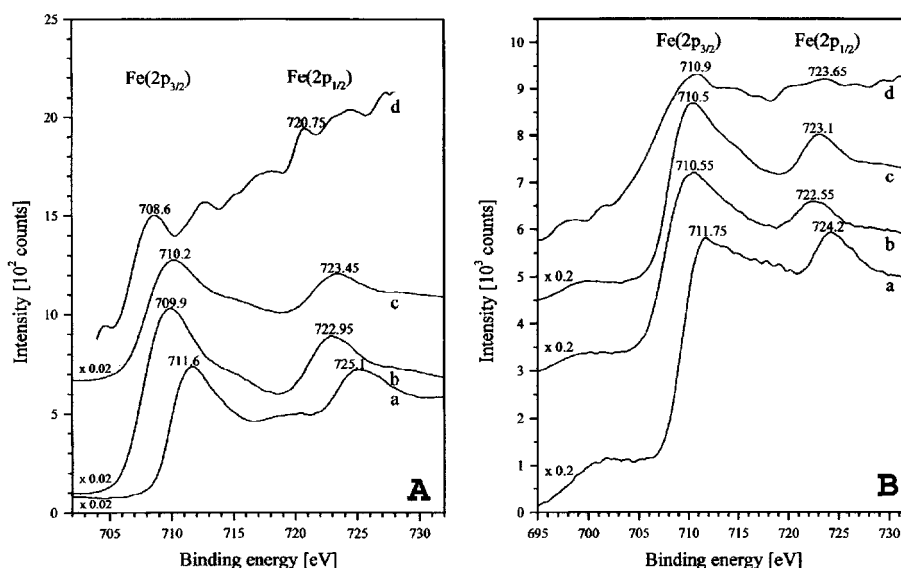
It is worth mentioning that after the reaction with acetylene, the sample was covered by soot, so the original spectrum was rather noisy and, hence, had to be heavily smoothed [Fig. 6(d)]. This process could also create and destroy minor spectrum characteristics. Nevertheless, there can be seen a small peak located at 712.7 eV and another one around 724 eV. The distance and the intensities of these peaks are characteristic of the Fe 2p doublet. As to the binding energy, the 712.7 eV value is about one eV higher than that accepted for  $\text{Fe}^{3+}$ . Obviously, the presence of an even more oxidized iron atom can be excluded. Instead, we suggest that during the high-temperature treatment, the chemical environment of a part of the iron atoms changed in a way that resulted in the apparently high binding energy doublet. It should be remembered that this high-binding energy means lower kinetic energy in fact.

In summary, we do conclude that during the high-temperature treatment, a part of the iron atoms formed alloy with Cobalt,

TABLE II

DATA EXTRACTED FROM MÖSSBAUER SPECTRA OF FRESH AND SPENT CATALYSTS (IS: ISOMER SHIFT, RELATIVE TO METALLIC  $\alpha$ -IRON, mm/s; QS: QUADRUPOLE SPLITTING, mm/s; MHF: INTERNAL MAGNETIC HYPERFINE FIELD, TESLA; RI: SPECTRAL CONTRIBUTION, %)

Sampl	Comp.	Fe/Al <sub>2</sub> O <sub>3</sub>				Fe,Co/Al <sub>2</sub> O <sub>3</sub>			
		IS	QS	MHF	RI	IS	QS	MHF	RI
Fresh (77 K)	Fe <sup>3+</sup> (A)	0.38	-	50.9	28	0.41	-	50.5	36
	Fe <sup>3+</sup> [B]	0.46	-	52.7	30	0.58	-	53.3	14
	Fe <sup>(2+)</sup> <sub>mi</sub>	0.76	-	47.3	16	0.53	-	43.6	14
	Fe <sup>3+</sup>	0.41	1.09	-	13	0.44	1.04	-	17
	Fe <sup>2+</sup>	1.04	2.52	-	12	1.02	2.38	-	19
Spent (77 K)	Fe <sub>metal</sub>	0.12	-	33.8	24	0.14	-	33.6	19
	FeCo <sub>alloy</sub>	0.14	-	-	-	0.14	-	34.5	62
	Θ-Fe <sub>3</sub> C	0.32	-	24.3	58	-	-	-	-
	Fe <sup>2+/3+</sup>	0.79	1.29	-	9	-	-	-	-
	Fe <sup>2+</sup>	1.16	2.54	-	8	1.16	2.51	-	10
Spent (300)	Fe <sub>metal</sub>	0.02	-	33.0	29	0.04	-	33.4	27
	FeCo <sub>alloy</sub>	0.03	-	-	-	0.03	-	34.3	51
	Θ-Fe <sub>3</sub> C	0.21	-	20.4	49	-	-	-	-
	Fe <sup>2+</sup>	0.91	1.98	-	9	0.92	1.79	-	10
	Fe <sup>3+</sup>	0.42	0.46	-	10	0.25	0.68	-	12

Fig. 6. XPS spectra of Fe/Al<sub>2</sub>O<sub>3</sub> (A) and 5%Fe+5%Co/Al<sub>2</sub>O<sub>3</sub> (B) in Fe(2p) region. (a) After evacuation at 300 K for 60 min. (b) After calcination at 1000 K for 20 min. (c) After 20 torr C<sub>2</sub>H<sub>4</sub> adsorption at 300 K for 60 min. (d) After interaction with 20 torr C<sub>2</sub>H<sub>4</sub> at 1000 K for 60 min.

while the rest got into a changed chemical environment of the substrate.

In order to obtain more information about the large quantity of carbon formed on bimetallic catalyst at 1000 K, the C(1s) was also monitored by XPS. The measured 284.65 eV binding energy is higher than that of the carbidic carbon measured on Fe/Al<sub>2</sub>O<sub>3</sub>. This value is close to that of graphitic carbon, but it is also close to the value measured in the interaction of C<sub>60</sub>, fullerene, and carbon nanotube with Ar ion beam [23].

#### IV. CONCLUSION

The intimate mixing of Co and Fe took part already in the first stage: mixed Fe,Co spinel formed as it was clearly demonstrated in the Mössbauer spectra. During the reaction, this spinel oxide precursors were converted into a catalytically

active form. It was clearly demonstrated that in this step zerovalent components were formed, namely, Θ-Fe<sub>3</sub>C on the Fe/Al<sub>2</sub>O<sub>3</sub>, whereas carbide formation did not take place in the Fe,Co; instead, bimetallic Fe,Co alloy was observed. In addition, the presence of iron can be detected in minor amounts in both the Fe and Fe,Co samples. These features are in good agreement with the literature data observed on other catalytic systems, e.g., Fischer-Tropsch's reaction (CO+H<sub>2</sub>); it was proven that the addition of cobalt to the iron containing catalysts suppressed the formation of iron carbides [24].

To identify a phase by XRD and by Mössbauer (for the appearance of magnetically ordered phase) a minimal size of phases is necessary. This critical size is the same range for the two methods (~6–8 nm), although it is slightly larger for XRD.

Thus, the slight discrepancy (XRD exhibits still spinel, whereas Mössbauer confirms the dominating presence of

Fe,Co bimetallic particles) can tentatively be explained as follows: XRD provides information on slightly larger regions than the Mössbauer spectroscopy, thus, the particle size of bimetallic Fe,Co may be in the 6- to 12-nm range. This is in good correlation with the general inner diameter of the formed carbon nanotubes.

Summarizing the results obtained in the catalytic synthesis of carbon nanotubes by Fe and Fe,Co supported on  $Al_2O_3$ , it can be stated that all the catalysts used are able to produce nanotubes, however, high activity and selectivity can be achieved using only the bimetallic sample. Mössbauer spectroscopy and XPS proved that on the bimetallic sample Fe,Co alloy was formed during the reaction and the carbon deposit was graphitic, while on the iron containing the monometallic catalyst, carbidic deposit was generated and carbon fibers were formed predominantly over this catalyst.

## REFERENCES

- [1] S. Iijima, "Helical microtubules of graphitic carbon," *Nature*, vol. 354, pp. 56–58, 1991.
- [2] T. W. Ebbesen, H. J. Lezec, H. Hiura, J. W. Bennett, H. F. Ghaemi, and T. Thio, "Electrical conductivity of individual carbon nanotubes," *Nature*, vol. 382, pp. 54–56, 1996.
- [3] R. S. Ruoff and D. C. Lorents, "Mechanical and thermal properties of carbon nanotubes," *Carbon*, vol. 33, pp. 925–930, 1995.
- [4] A. Thess, R. Lee, P. Nikolaev, P. Dai, P. Petit, J. Robert, C. Xu, Y. H. Lee, S. G. Kim, A. G. Rinzler, D. T. Colbert, G. E. Scuseria, D. Tomanek, J. E. Fisher, and R. E. Smalley, "Crystalline ropes of metallic carbon nanotubes," *Science*, vol. 273, pp. 483–487, 1996.
- [5] T. W. Ebbesen and P. M. Ajayan, "Large-scale synthesis of carbon nanotubes," *Nature*, vol. 358, pp. 220–222, 1992.
- [6] V. Ivanov, J. B. Nagy, Ph. Lambin, A. Lucas, X. B. Zhang, X. F. Zhang, D. Bernaerts, G. Van Tendeloo, S. Amelinckx, and J. Van Landuyt, "The study of carbon nanotubes produced by catalytic method," *Chem. Phys. Lett.*, vol. 223, pp. 329–335, 1994.
- [7] K. Mukhopadhyay, A. Koshio, T. Sugai, N. Tanaka, H. Shinohara, Z. Kónya, and J. B. Nagy, "Bulk production of quasi-aligned carbon nanotube bundles by the catalytic chemical vapor deposition (CCVD) method," *Chem. Phys. Lett.*, vol. 303, pp. 117–124, 1999.
- [8] A. M. Zhang, C. Li, S. L. Bao, and Q. H. Xu, "A novel method of varying the diameter of carbon nanotubes formed on an Fe-supported Y zeolite catalyst," *Microporous Mesoporous Mater.*, vol. 29, pp. 383–388, 1999.
- [9] I. Willems, Z. Kónya, J.-F. Colomer, G. Van Tendeloo, N. Nagaraju, A. Fonseca, and J. B. Nagy, "Control of the outer diameter of thin carbon nanotubes synthesized by catalytic decomposition of hydrocarbons," *Chem. Phys. Lett.*, vol. 317, pp. 71–76, 2000.
- [10] P. Coquay, R. E. Vandenberghe, E. De Grave, A. Fonseca, P. Piedigrosso, and J. B. Nagy, "X-ray diffraction and Mossbauer characterization of an Fe/SiO<sub>2</sub> catalyst for the synthesis of carbon nanotubes," *J. Appl. Phys.*, vol. 2, pp. 1286–1291, 2002.
- [11] A. K. M. F. Kibria, Y. H. Mo, and K. S. Nahm, "Synthesis of carbon nanotubes over nickel-iron catalysts supported on alumina under controlled conditions," *Catal. Lett.*, vol. 71, pp. 229–236, 2001.
- [12] D. Gournis, M. A. Karakassides, T. Bakas, N. Boukos, and D. Petridis, "Catalytic synthesis of carbon nanotubes on clay minerals," *Carbon*, vol. 40, pp. 2641–2646, 2002.
- [13] K. Hernadi, A. Fonseca, J. B. Nagy, D. Bernaerts, and A. A. Lucas, *Carbon*, vol. 34, p. 1249, 1996. K. Hernadi, A. Fonseca, J. B. Nagy, A. Siska, I. Kiricsi, "Production of nanotubes by the catalytic decomposition of different carbon-containing compounds," *Appl. Catal. A: Gen.*, 199, pp. 245–255, 2000.
- [14] J. F. Colomer, P. Piedigrosso, I. Willems, C. Journet, C. Bernier, G. Van Tendeloo, A. Fonseca, and J. B. Nagy, "Purification of catalytically produced multi-wall nanotubes," *J. Chem. Soc. Faraday Trans.*, vol. 94, pp. 3753–3758, 1998.
- [15] I. Vesselőnyi, K. Niesz, A. Siska, Z. Kónya, K. Hernádi, J. B. Nagy, and I. Kiricsi, "Production of carbon nanotubes on different metal supported catalysts," *React. Kinet. Catal. Lett.*, vol. 74, pp. 329–336, 2001.
- [16] Á. Kukovecz, Z. Kónya, N. Nagaraju, I. Willems, A. Tamási, A. Fonseca, J. B. Nagy, and I. Kiricsi, "Catalytic synthesis of carbon nanotubes over Co, Fe and Ni containing conventional and sol-gel silica-aluminas," *Phys. Chem.*, vol. 2, pp. 3071–3076, 2000.
- [17] Z. Kónya, "Catalytic production, purification, characterization and application of single- and multiwall carbon nanotubes," in *NATO-ASI Carbon Filaments and Nanotubes: Common Origins, Differing Applications?*, L. P. Biró, C. A. Bernardo, G. G. Tibbets, and Ph. Lambin, Eds. Norwell, MA: Kluwer, 2001, pp. 85–109.
- [18] R. E. Vandenberghe and E. De Grave, *Mössbauer Spectroscopy Applied to Inorganic Chemistry*. Norwell, MA: Kluwer, 1985, p. 59.
- [19] J. W. Niemantsverdriet, A. M. van der Kraan, W. L. van Dijk, and H. S. van der Baan, "Behavior of metallic iron catalysts during Fischer-Tropsch synthesis studied with Mossbauer-spectroscopy, X-ray-diffraction, carbon content determination, and reaction kinetic measurements," *J. Phys. Chem.*, vol. 84, pp. 3363–3370, 1980.
- [20] B. S. Clausen and H. Topsoe, "Preparation and properties of small silica-supported iron catalyst particles—Influence of reduction procedure," *Appl. Catal.*, vol. 48, pp. 327–339, 1989.
- [21] G. C. Allen, M. T. Curtis, A. J. Hooyer, and P. M. Tucker, "X-Ray photoelectron spectroscopy of iron-oxygen systems," *J. Chem. Soc., Dalton Trans.*, pp. 1525–1530, 1974.
- [22] D. J. Duvenhage and N. J. Coville, "Fe:Co/TiO<sub>2</sub> bimetallic catalysts for the Fischer-Tropsch reaction I. Characterization and reactor studies," *Appl. Catal. A-Gen.*, vol. 153, pp. 43–67, 1997.
- [23] Y. Zhu, T. Yi, B. Zheng, and L. Cao, "The interaction of C-60 fullerene and carbon nanotube with Ar ion beam," *Appl. Surf. Sci.*, vol. 137, pp. 83–90, 1999.
- [24] T.-A. Lin, L. H. Schwartz, and J. B. Butt, "Iron Alloy Fischer-Tropsch Catalyst 5. FeCo on Y-zeolite," *J. Catal.*, vol. 97, pp. 177–187, 1986.



**Zoltán Kónya** received the M.Sc. and Ph.D. degrees in chemistry and environmental sciences from the University of Szeged, Szeged, Hungary, in 1994 and 1998, respectively.

Following postdoctoral research at the Universitair Notre-Dame de la Paix, Universitair de Namur, Universitair de Belgium, and the University of California, Berkeley, he joined University of Szeged, where he is currently an Associate Professor with the Applied and Environmental Chemistry Department. His current research interests include the nanosize metal and semiconductor structures—their synthesis, characterization, and applications.



**István Vesselőnyi** received the B.A. and M.A. degrees in environmental engineering from the University of Oradea, Oradea, Romania, in 2000, and is currently working toward the Ph.D. degree at the University of Szeged, Szeged, Hungary.

His current research interests include the synthesis, characterization, and application of multiwall carbon nanotubes.



**Károly Lázár** received the chemistry degree from Eötvös Loránd University, Budapest, Hungary, in 1971 and the Ph.D. degree from the Central Research Institute for Physics, Budapest, in 1975.

In 1979, he joined the Mössbauer Laboratory established at that time at the Catalysis Department of the Institute of Isotopes, Budapest, where he is currently the Head of the Mössbauer Laboratory and the Department of Catalysis and Tracer Studies. Since the mid-1990s, his research interests have been in the studies of the micro- and mesoporous systems, containing iron and tin incorporated into the porous matrix. He is coauthor of 110 publications.



**János Kiss** received the M.Sc. and Ph.D. degrees in chemistry from József Attila University, Szeged, Hungary, in 1972 and 1976, respectively, and the D.Sc. degree in chemistry from the Hungarian Academy of Sciences, Budapest, in 1993.

His current research interests include the surface science, solid-gas interactions and dynamics, photo-induced surface processes, characterization of adsorbed species and surface intermediates, catalysis, electron spectroscopy (Auger, XPS, UPS, and ELS), and infrared spectroscopy (RAIRS).



**Imre Kiricsi** received the M.Sc. and Ph.D. degrees in chemistry from the József Attila University, Szeged, Hungary, in 1972 and 1975, respectively, and the D.Sc. degree in chemistry from the Hungarian Academy of Sciences, Budapest, in 1992.

In 1985 and 1986, he was an Alexander von Humboldt Fellow with the University of Hamburg, Hamburg, Germany. From 1992 and 1993, he was a Consultant with Eniricerche SpA, Milano, Italy. In 2002, he was a Visiting Professor with the University of California, Berkeley. He is currently a Professor of Applied and Environmental Chemistry at the University of Szeged. He is the holder of several patents in zeolite chemistry, and has coauthored over 300 journal papers, books, and book chapters related to micro-, mezo-, and macroporous materials.

Dr. Kiricsi is President of the Hungarian Zeolite Association and the Catalysis Club of the Hungarian Academy of Sciences.